

# A Preliminary Result on Electrical Capacitance Tomography for Gas-solid Flow in Pneumatic Conveyor System.

Nur Arina Hazwani Samsun Zaini<sup>1</sup>, Ruzairi Abdul Rahim<sup>1\*</sup>, Herman Wahid<sup>1</sup>, Juliza Jamaludin<sup>2</sup>, Mimi Faisyalini Ramli<sup>3</sup>, Nasarudin Ahmad<sup>1</sup>, Mohamad Shukri Abdul Manaf<sup>1</sup>, Yusri Md. Yunos<sup>1</sup>, Anita Ahmad<sup>1</sup>, Ahmad Azahari Hamzah<sup>5</sup>, Chan Kok San<sup>4</sup>, Farah Aina Jamal Mohamad<sup>1</sup>, and Navintiran Rajan<sup>1</sup>

<sup>1</sup>Faculty of Electrical Engineering, Universiti Teknologi Malaysia, 81310 UTM Skudai, Johor, Malaysia.

<sup>2</sup>Faculty of Engineering and Built Environment, Universiti Sains Islam Malaysia, 71800 Negeri Sembilan, Malaysia.

<sup>3</sup>Faculty of Technology Engineering, Universiti Tun Hussein Onn, Campus Pagoh, Johor, Malaysia.

<sup>4</sup>I-Stone Technology Sdn. Bhd, Senai, Johor, Malaysia.

<sup>5</sup>Section of Chemical Engineering Technology, UniKL MICET, 78000, Alor Gajah, Melaka, Malaysia.

\*Corresponding author: ruzairi@fke.utm.my, Tel: 607-5535310, Fax: 607-5566272

**Abstract:** Electrical capacitance tomography (ECT) is categorized as a soft-field sensor which is non-invasive and non-intrusive instrument that can provide the visualization of cross-sectional distribution of any kind of multiphase flow. ECT would help in understanding the gas-solid flow interaction. This research is conducted to overcome some difficulties in measurement of gas-solid flows that exist in multiphase flows in pipelines or vessels such as the sedimentation of the solid and the velocity of the solid particles. Hence, the characterization of gas-solid two-phase flow by implementing an ECT system is necessary. Three objectives are set for this research which are the determination of an optimum frequency and amplitude for capacitance measurement of Poly-methyl methacrylate (PMMA) material by ECT system, the determination of the average solid velocity in gas-solid two-phase flow through cross-correlation method using Parseval's theorem, and image reconstruction based on eight ECT sensors using Linear Back Projection (LBP) algorithm. This paper concise the theory of ECT system, existing works, proposed methodology, and the expected results.

**Keywords:** ECT, gas-solid flow, cross-correlation, linear back projection.

© 2021 Penerbit UTM Press. All rights reserved

*Article History: received 25 Mei 2021; accepted 12 June 2021; published 15 October 2021.*

## 1. INTRODUCTION

The tomography systems had already begun in the medical field in 1950. The need for an instrument that is stable, non-invasive and can work with fast flowing fluid is significantly improved at that moment [1]. Tomography system had been applied in many sectors such as Chemical Engineering, Geophysics, Botanical fields, Powder technology, and many more [2]. According to Webster's dictionary, "tomography" is derived from the Greek word "tomos" [3]. It requires the use of tomographic imaging techniques to manipulate remote sensor data [4].

The accurate measurement of gas/solid flow parameters such as the velocity and flow regime are of great importance in improving product quality and production efficiency. The piping system in a pneumatic transport system plays an important role in many manufacturing processes. When designing a low-cost pneumatic transport system, it is important to understand the impact of variables like velocity, material distribution, flow regime, and others on the system's transport capability.

One of the basic criteria for the performance of such a transportation device is to maintain low air pressure during granular material propagation. As a result, real-time calculation of solid velocity in pneumatic transport will help to increase granular material transportation performance [5]. Insufficient particle velocity, on the other hand, often results in pipeline blockage and an unpredictable flow condition [6]. For pneumatic conveying systems, precise calculation of particle velocity is important [7].

This project will focus on the piping of the pneumatic conveying system of PMMA pellets. The measurement will take place in the highlighted part as illustrated in Figure 1 below. Pneumatic conveying of solid particles exists widely in thermal power, plastic, and the food industry [8].

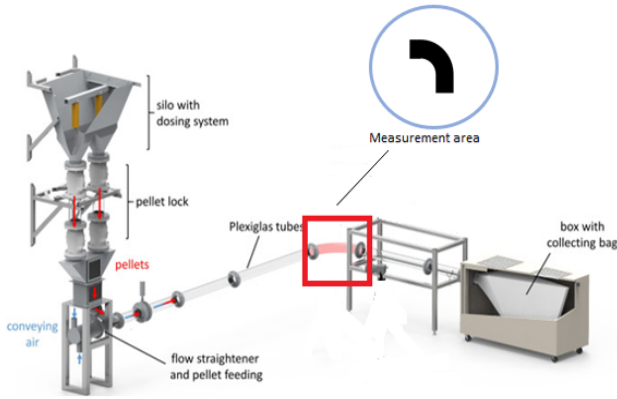


Figure 1. The illustration of the pneumatic conveying system [9]

Next, G. Heming et.al [7] designed and developed a novel solid particle velocimeter based on Differential Capacitance Sensor Array (DCSA). But in this work, they solely measure the velocity of the solid particle without doing the image reconstruction of the flow in the pneumatic conveying systems. From the current method, the characterization of gas-solid two-phase flow needs to adopt two different methods which can consume more time. The best technique in characterizing multiphase flow phenomena is by visualization method inside the system without invading the flow. This is because if the measuring process invades the flow in a pipe, it will disturb the process in the pipe flow. In this paper, there will be an implementation of both techniques. We can monitor the flow in the pneumatic conveyor and determine if there is a blockage in the pipe or vessel.

At the same time, we can also measure the velocity of the solid particle so that the performance of the system can be maintained. Tomography system, especially electrical capacitance tomography (ECT), offers a more versatile option to discover online flow phenomena non-invasive and non-intrusive. The simulation work will be conducted using COMSOL Multiphysics and MATLAB while the experimental work uses the ECT system. This study covered the designing of sensors arrays, velocity profile and velocity distribution determination in the frequency domain by applying Parseval's theorem, and image reconstruction by LBP algorithm for 8 ECT sensors.

## 2. ECT

Electrical Capacitance Tomography (ECT) is a soft-field sensor, which sensitivity decreases towards the pipe's middle. It detects the variation of permittivity distribution in the closed region or pipe. The ECT sensor consists of a variety of primary measurement electrodes, radial and axial end of screen's ends, an external insulation frame, connectors, and coaxial cable. Usually, the ECT system will consist of between 8 or 12 electrodes [10]. The typical ECT system configuration is shown in Figure 2 below.

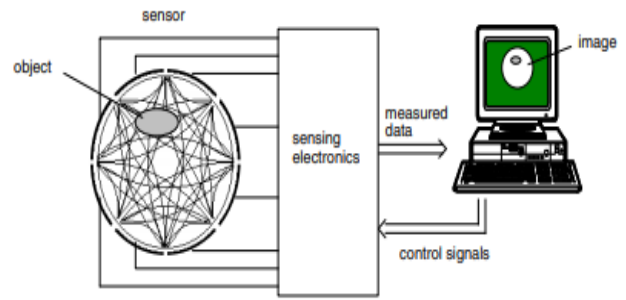


Figure 2. Typical ECT system configuration consists of eight-electrodes sensors [11]

### 2.1 Principles of ECT system

The core principle of the ECT system is to measure the capacitance shifts of the multiple electrode sensor and to utilize the computed capacitance values to recreate the permittivity distribution. In order to visualize the medium located in the pipes or vessel, several electrodes should be arranged along the boundaries of the area. Then, the capacitance between all the combination pairs of the electrodes can be determined. An image can be generated from the data obtained by using any suitable reconstruction algorithm [12].

The basic ECT system can consist of several numbers of 8, 12, or 16 electrodes, a capacitance measurement circuit, a central control unit, and a control PC. The signal conditioning system consists of amplifying circuit, filter circuit, AC to DC converter circuit, and capacitance measurement circuit [13]. Figure 3 shows the cross-sectional view of the ECT sensor.

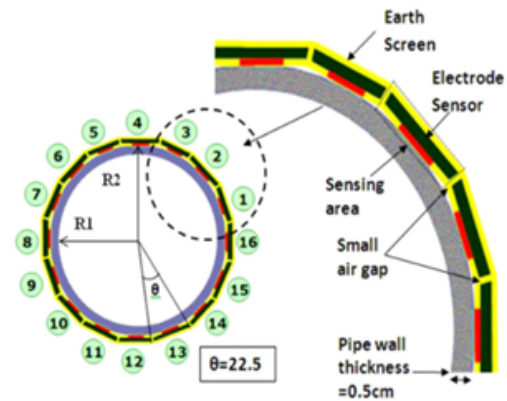


Figure 3. Cross-sectional view of ECT sensor [14]

Between any two electrodes, the mutual capacitance is determined where one active electrode acts as a transmitter and the other grounded electrodes function as receivers. The number of independent capacitance measurements  $M$  for one distribution is given by Equation (1) below [15]:

$$M = \frac{N(N-1)}{2} \quad (1)$$

where  $M$  is the total collected capacitance measurements and  $N$  represents the number of the total electrodes.

### 2.2 ECT Applications

This section presents some existing ECT applications that involve Gas-solid multiphase flow. Table 1 below shows the ECT application with its limitations.

Table 1. ECT applications.

Ref .	No. of electrode	Parameter studies	Limitation
[16]	8 (dual planes)	Monitoring powder mixing by using ECT tomogram by LBP algorithm.	No blockage localization and velocity measurement of the solid particles.
[17]	16 (dual planes)	Calculate the sedimentation velocity by using the correlation function.	No visualization of the flow and blockage detection.
[18]	8 (single plane)	-In the case of water-dominated vertical flows. -The Landweber procedure, Tikhonov regularization method, and Linear Back Projection method, have been investigated.	No velocity measurement and LBP algorithm are faster compared to other image reconstruction algorithm.

### 3. METHODOLOGY

This section presents the proposed methodology for this research. This research will be divided into two parts which are the simulation and experimental parts.

#### 3.1 PMMA Material

PMMA is an adaptable type of plastic that can be used in a variety of fields and forms [19]. By looking into the manufacturing part, PMMA has been applied in many production processes such as glazing, commercial signs, eye lenses, fiber optics for light piping, solar panels, windows, skylights, and aquariums [20]. PMMA material can be in forms of molding compound beads or pellets, sheets and cast sheets as shown in Figure 4 below. PMMA pellets are shown in Figure 5 below. Some important parameters of the PMMA material are shown in Table 2.

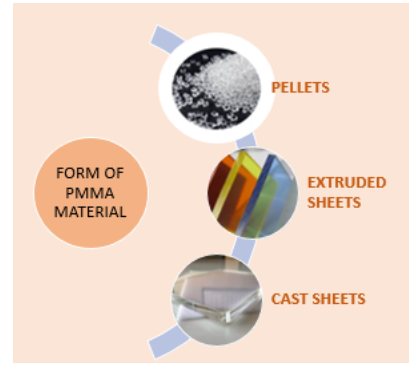


Figure 4. Forms of PMMA material.



Figure 5. PMMA pellets.

Table 2. PMMA material parameters [21].

PARAMETERS	PMMA
Chemical Formula	$C_5O_2H_8$
Refractive Index	1.49
Melting Point ( $^{\circ}C$ )	160
Density ( $g/cm^3$ )	1.2

#### 3.2 Image Reconstruction Algorithm

Image reconstruction is the process used to produce a picture or an image within a region, from the data obtained on its boundary non-invasively [22].

##### 3.2.1 LBP Algorithm

LBP algorithm was categorized as non-iterative algorithms [23][24]. The non-iterative algorithm also known as the single-step algorithm in which it does not have the repetition of the process. For non-iterative algorithms, the famous and commonly used algorithms are Linear Back Projection (LBP), Tikhonov regularization, Direct method based on singular value decomposition, and multiple linear regression and regularization [11]. The Linear Back Projection is described in Equation (2) below:

$$G = S^T C \quad (2)$$

where G is the value of normalized permittivity distribution (F/m),  $S^T$  is the value matrix transpose of sensitivity map distributions (1/m) and C is the value of normalized capacitance measurement (F).

### 3.4 Simulation

The simulation works involved the implementation of Comsol Multiphysics and Matlab software. This part aimed to calculate the accuracy of the image reconstruction of eight ECT sensors using the LBP algorithm and to study the effectiveness of the Parsevals theorem in calculating time lag. Figure 6 below shows the configuration of the Electrical Capacitance sensor. The specification or the parameter for the simulation works is shown in Table 3 below.

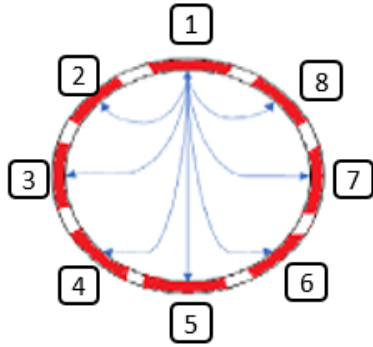


Figure 6. ECT with eight electrodes.

Table 3. Specification for ECT sensor.

PARAMETER	VALUE
INNER PIPE DIAMETER (mm)	45
OUTER PIPE DIAMETER (mm)	50
NO. OF ELECTRODE, N	8
SIGNAL AMPLITUDE, $V_{PP}$ (V)	16
FREQUENCY, $f$ (kHz)	160
PERMITTIVITY	Acrylic pipe (2.6) Air (1)

### 3.5 Experimental Setup

The experimental works will start with designing the twin planes 8-electrodes ECT system by using the COMSOL Multiphysics software. Next, the best or optimum frequency and amplitude for the ECT system will be determined by carrying out some experiments with PMMA material. Then, the solid velocity measurement of the PMMA pellets will be carried out. Lastly, the visualization of the image in the pipe or vessel will be done using the LBP algorithm.

#### 3.5.1 Optimum Frequency and Amplitude.

For the determination of optimum frequency and amplitude, the experiment will be divided into two parts which are the static and dynamic experiments. The

frequency and amplitude dependence experiment will be conducted in order to obtain the optimal combination of frequency and amplitude for the ECT system to measure PMMA material.

In the static experiment, a suitable frequency range will be obtained, while in the dynamic experiment, we determined the optimal frequency. The setup of the static experiment involved eight channels of ECT sensors, an impedance analyzer, a multiplexer, and a personal computer, as shown in Figure 7 below. The setup for optimal frequency is shown in Figure 8 below.

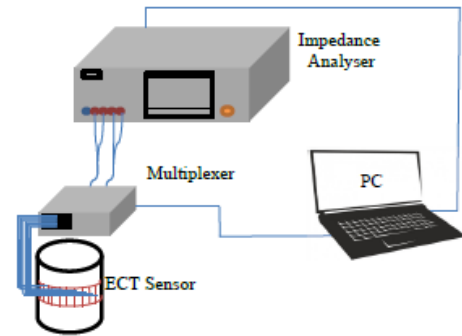


Figure 7. Experimental setup for static experiment.

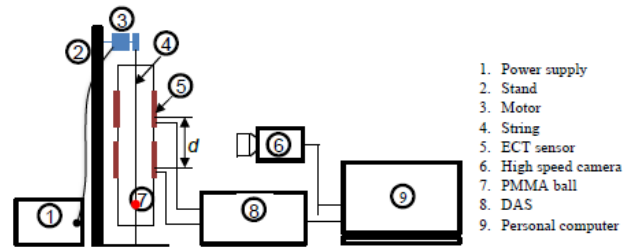


Figure 8. Experimental setup for dynamic experiment.

The first parameter considered is the frequency, and the second parameter considered was the amplitude,  $V_{p-p}$ . For the dynamic experiment, the velocity will be analyzed using the previous cross-correlation method which was the direct correlator (DC) and average square different function (ASDF) for a variety of frequency values based on the results of the static experiment. The amplitude,  $V_{p-p}$  will be measured using the same setup in Figure 8. The optimal frequency obtained from the frequency dependence experiment will be used with a range of amplitudes  $V_{p-p}$ .

#### 3.5.2 Velocity Measurement.

An experiment will be conducted to investigate the average velocity of the PMMA pellets in the piping system. Parseval's theorem will be used under the optimal conditions for the AC-ECT system for the measurement of data, and the LBP algorithm will be applied for image reconstruction. The last part aimed to measure the average velocity of PMMA pellets in the circulating piping system based on the optimum frequency and amplitude obtained. The time lag and average velocity will be calculated using MATLAB.

**4. PRELIMINARY RESULTS.**

A simple capacitor simulation in COMSOL Multiphysics was carried out. This simulation includes the designing process of a capacitor, the meshing process, and the 3D plotting. All the parameters for the metal, ground boundary, and terminal boundary parts were set to a specific value in order to create the 3D representation or image of the capacitor model. The medium located between the capacitor plates is Air. The permittivity value for Air is 1.

The explicit, blue-colored sections in Figure 9 (a) are the metal part referring to the capacitor part. Then, the mesh rendering was done as shown in Figure 9 (b). The meshing process is important in any simulation process because the mesh influences the simulation's precision, convergence, and pace.

Maxwell capacitance (F)  
1.6830E-10

Figure 10. Capacitor output value.

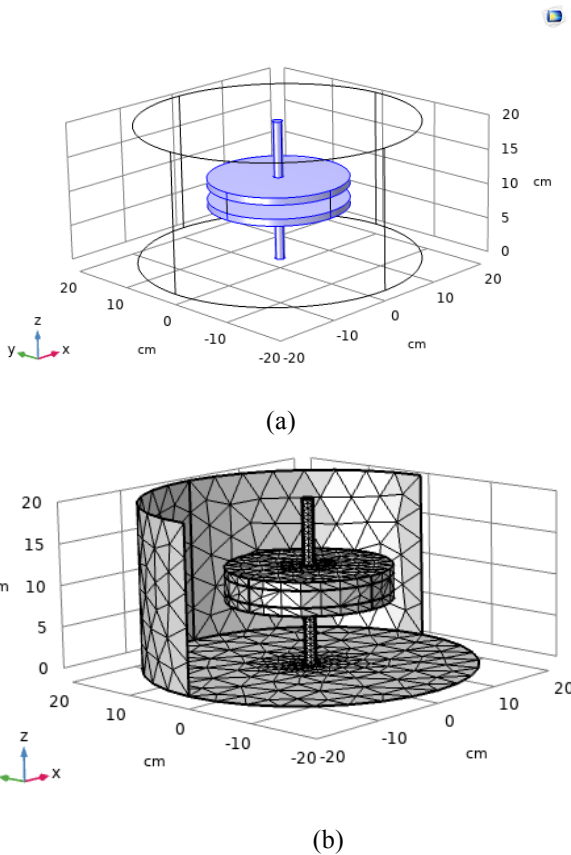


Figure 9. (a): Capacitor model, (b): Meshing process.

The global evaluation produced the value of the capacitor as shown in Figure 10 below. The 3D representation of electric potential (V) and electric field are shown in Figure 11 below. The arrow in Figure 11 represents the electric field flow around the capacitor plates. The electric field is a vector field that represents the interaction between the charge of a test particle inserted into the field and the force imposed on it. The purpose of this preliminary simulations is to show the basic theory behinds electrical capacitance sensor.

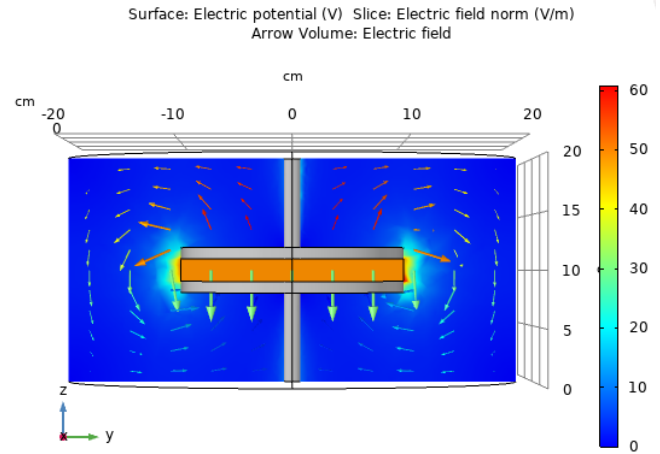


Figure 11. 3D representation of electric potential (V) and electric field.

**5. CONCLUSION AND FUTURE WORKS**

The work presented in this paper offers opportunities for further study in several areas. ECT is the best tool to monitor the solid-gas flow in a pneumatic conveyor piping system due to its non-invasive and non-intrusive properties. The monitoring process of multiphase flow is important to prevent the occurrence of blockage in the piping system which will affect the production and system efficiency. Future work that needs to be done is the modelling of an actual ECT system that binds on the outer of the pipe. Next, the simulation process in COMSOL Multiphysics will be done to evaluate the LBP algorithm accuracy and to study the effectiveness of the Parsevals theorem in calculating time lag. Lastly, the measurement of the average velocity of PMMA pellets will be carried out through some experiments as mentioned in the proposed methodology.

**ACKNOWLEDGMENT**

The authors would like to thank to Universiti Teknologi Malaysia for supporting the research study under UTMER Research Fund, vot number QJ130000.3851.19J61

**REFERENCES**

[1] M. S. Beck, T. Dyakowski, and R. A. Williams, "Process tomography - the state of the art," *Trans. Inst. Meas. Control*, vol. 20(4), 1998, pp. 163–177.  
 [2] J. Jamaludin et al., "A Review of Tomography System," *Jurnal Teknologi*, vol. 64(5), 2013, pp. 2180–3722.



- [3] J. Hsieh, "Computed Tomography: Principles, Design, Artifacts, and Recent Advances", *Published by SPIE – The International Society for Optical Engineering*, 2003.
- [4] S.M. Huang, C.G.Xie, J.A.Salkeld, A.Plaskowski, R.Thorn, R.A.Williams, A. Hunt, M.S. Beck, *Process tomography for identification, design and measurement in industrial systems*, Science Direct, 1992, pp. 85-92.
- [5] A. Hashim, "Recent Review on Poly-methyl methacrylate (PMMA)- Polystyrene (PS) Blend Doped with Nanoparticles For Modern Applications," *Res. J. Agric. Biol. Sci.*, no. December, 2019, pp. 2–9.
- [6] Y. Yan, "Mass flow measurement of bulk solids in pneumatic pipelines," *Measurement Science and Technology*, 1996, Vol. 7(12), pp. 1687-1706.
- [7] G. Heming, D. Huiwen, M. Yingxing, W. Bing, and F. Bingyan, "Local solid particle velocity measurement based on spatial filter effect of differential capacitance sensor array," *J. Eng.*, vol. 2019(23), 2019, pp. 9195–9200.
- [8] M. P. Mathur and G. E. Klinzing, "Flow measurement in pneumatic transport of pulverized coal," *Powder Technol.*, 1984, vol. 40, no. 1–3, pp. 309–321.
- [9] J. Jägers, S. Wirtz, V. Scherer, and M. Behr, "Experimental analysis of wood pellet degradation during pneumatic conveying processes," *Powder Technol.* 2020, vol. 359, pp. 282–291.
- [10] N. Amizan *et al.*, "A Review on Electrical Capacitance Tomography Sensor Development," *J. Teknol.*, 2015, vol. 3(73), pp. 35–41.
- [11] Y. Li, S. Cao, Z. Man, and H. Chi, "Image reconstruction algorithm for electrical capacitance tomography," *Inf. Technol. J.*, 2011, vol. 10(8), pp. 1614–1619.
- [12] Ruzairi Abdul Rahim, *Electrical Capacitance Tomography Principal, Techniques and Applications*. Johor Bahru: Penerbit UTM Press, 2011.
- [13] W. Yang, "Key issues in designing capacitance tomography sensors," *Proc. IEEE Sensors*, 2006, pp. 497–505.
- [14] E. J. Mohamad, R. A. Rahim, M. H. F. Rahiman, H. L. M. Ameran, S. Z. M. Muji, and O. M. F. Marwah, "Measurement and analysis of water/oil multiphase flow using Electrical Capacitance Tomography sensor," *Flow Meas. Instrum.*, 2016, vol. 47, pp. 62–70.
- [15] W. Deabes, A. Sheta, K. E. Bouazza, and M. Abdelrahman, "Application of electrical capacitance tomography for imaging conductive materials in industrial processes," *J. Sensors*, 2019, pp 1-23. doi <https://doi.org/10.1155/2019/4208349>
- [16] G. Forte, P. J. Clark, Z. Yan, E. H. Stitt, and M. Marigo, "Using a Freeman FT4 rheometer and Electrical Capacitance Tomography to assess powder blending," *Powder Technology*, 2018, vol. 337, pp. 25–35.
- [17] V. Mosorov, M. Zych, R. Hanus, D. Sankowski, and A. Saoud, "Improvement of flow velocity measurement algorithms based on correlation function and twin plane electrical capacitance tomography," *Sensors*, 2020, vol. 20(1), 306.
- [18] M. S. Hossain, M. Towsif Abir, and M. A. Islam, "A Comparative Study of Different Methods using Electrical Capacitance Tomography for Water-Dominated Multiphase Vertical Flows," *2019 IEEE Int. Conf. Signal Process. Information, Commun. Syst. SPICSCON 2019*, 2019, pp. 36–39.
- [19] U. Ali, K. J. B. A. Karim, and N. A. Buang, "A Review of the Properties and Applications of Poly (Methyl Methacrylate) (PMMA)," *Polymer Reviews*, 2015, vol. 55(4), pp. 678–705.
- [20] A. M. A. Youssef, "Poly Methyle Metha Acrylate (Pmma)," *Prop. PMMA*, 2019, pp. 1–4.
- [21] F. W. Billmeyer, "Textbook of Polymer Science," *Kobunshi*, vol. 12(3), 1963, pp. 240–251.
- [22] M. Moscoso, "Introduction to image reconstruction," *Lect. Notes Math.*, 2008, vol. 1943, pp. 1–16.
- [23] A. A. Hamzah *et al.*, "Simulation studies on image reconstruction algorithm for portable electrical capacitance tomography," *Int. J. Integr. Eng.*, 2018, vol. 10(8), pp. 107–111.
- [24] H. Yan, Y. F. Wang, and Y. G. Zhou, "Three-dimensional electrical capacitance tomography reconstruction by the Landweber iterative algorithm with fuzzy thresholding," *IET Sci. Meas. Technol.*, 2014, vol. 8(6), pp. 487–496.